Article

Functional Copy-Number Alterations as Diagnostic and Prognostic Biomarkers in Neuroendocrine Tumors

Hayley Vaughn [1,2], Heather Major [2], Evangeline Kadera [2], Kendall Keck [3], Timothy Dunham [2], Qining Qian [2], Bartley Brown [4], Aaron Scott [3], Andrew M. Bellizzi [5], Terry Braun [1,4], Patrick Breheny [6], Dawn E. Quelle [7], James R. Howe [3] and Benjamin Darbro [1,2,*]

1   Interdisciplinary Graduate Program in Genetics, University of Iowa, Iowa City, IA 52242, USA;
    hayley-vaughn@uiowa.edu (H.V.); terry-braun@uiowa.edu (T.B.)
2   Stead Family Department of Pediatrics, University of Iowa Health Care, Iowa City, IA 52242, USA;
    heather-major@uiowa.edu (H.M.); evangeline-kadera@uiowa.edu (E.K.); timothy-dunham@uiowa.edu (T.D.);
    qining-qian@uiowa.edu (Q.Q.)
3   Department of Surgery, University of Iowa Health Care, Iowa City, IA 52242, USA;
    kendall-keck@uiowa.edu (K.K.); aaron-scott@uiowa.edu (A.S.); james-howe@uiowa.edu (J.R.H.)
4   Department of Biomedical Engineering, University of Iowa, Iowa City, IA 52242, USA;
    bartley-brown@uiowa.edu
5   Department of Pathology, University of Iowa, Iowa City, IA 52242, USA; andrew-bellizzi@uiowa.edu
6   Department of Biostatistics, University of Iowa, Iowa City, IA 52242, USA; patrick-breheny@uiowa.edu
7   Department of Neuroscience and Pharmacology, University of Iowa, Iowa City, IA 52242, USA;
    dawn-quelle@uiowa.edu
*   Correspondence: benjamin-darbro@uiowa.edu

Abstract: Functional copy-number alterations (fCNAs) are DNA copy-number changes with concordant differential gene expression. These are less likely to be bystander genetic lesions and could serve as robust and reproducible tumor biomarkers. To identify candidate fCNAs in neuroendocrine tumors (NETs), we integrated chromosomal microarray (CMA) and RNA-seq differential gene-expression data from 31 pancreatic (pNETs) and 33 small-bowel neuroendocrine tumors (sbNETs). Tumors were resected from 47 early-disease-progression (<24 months) and 17 late-disease-progression (>24 months) patients. Candidate fCNAs that accurately differentiated these groups in this discovery cohort were then replicated using fluorescence in situ hybridization (FISH) on formalin-fixed, paraffin-embedded (FFPE) tissues in a larger validation cohort of 60 pNETs and 82 sbNETs (52 early- and 65 late-disease-progression samples). Logistic regression analysis revealed the predictive ability of these biomarkers, as well as the assay-performance metrics of sensitivity, specificity, and area under the curve. Our results indicate that copy-number changes at chromosomal loci 4p16.3, 7q31.2, 9p21.3, 17q12, 18q21.2, and 19q12 may be used as diagnostic and prognostic NET biomarkers. This involves a rapid, cost-effective approach to determine the primary tumor site for patients with metastatic liver NETs and to guide risk-stratified therapeutic decisions.

Keywords: neuroendocrine tumors; functional copy-number alterations; fluorescence in situ hybridization; diagnostic biomarkers; risk-stratifying biomarkers

1. Introduction

Neuroendocrine tumors (NETs) are epithelial neuroendocrine neoplasms with high metastatic potential. Up to 60% of patients have advanced metastatic liver disease at the time of diagnosis [1,2]. Primary NETs in the abdomen are regularly missed due to small tumor size, body habitus, and limitations of abdominal imaging [1]. Twelve to fifty percent of primary gastroenteropancreatic NETs (GEP NETs) go undetected by imaging [2].

GEP NETs that originate in the pancreas (pNETs) and small bowel (sbNETs) comprise half of all GEP NETs [3]. The two tumor sites cause similar signs and symptoms, including

abdominal pain, nausea, poor appetite, weight loss, and diarrhea [3]. Distinguishing between these two primary sites is important for guiding proper clinical management.

The incidence of GEP NETs is 3.56 per 100,000 people [3], but there remains a relatively high proportion of tumors that have an unknown primary site (0.86 per 100,000 people) [3]. While the incidence of sbNETs is twice as high as that of pNETs (12,000 vs. 6000 cases annually in the United States), pNETs are more aggressive, with a 5-year survival of 50% compared to 69% for sbNETs [3,4]. Treatment options for Grade 1 or Grade 2 (G1/G2) pNETs include surgery, somatostatin analogues (SSAs) [5], peptide-receptor radionuclide therapy (PRRT) [6], everolimus (an mTOR inhibitor) [7–9], sunitinib [10] (a VEGF inhibitor), and capecitabine/temozolomide chemotherapy [11,12]. There is limited consensus on the order of treatment when patients have progressive disease (PD). Treatment options for G1/G2 sbNETs include surgery, PRRT, and everolimus [5,6,13]. Treatment order is more established in sbNETs, with SSAs being the primary treatment, followed by PRRT and then everolimus for PD.

Immunohistochemistry is routinely used to infer site of origin in metastatic NETs of occult origin [14–16]. The most commonly employed markers include CDX2 (midgut) [17], polyclonal PAX8 (pancreas) [18], TTF-1 (lung) [19], and SATB2 (rectum) [20]. None of these are NET-specific, though, and all were adapted for this purpose from more widespread use as markers of adenocarcinoma site of origin [21]. Because of the infrequency of NETs relative to other malignant epithelial tumors, complementary (serotonin for midgut) or best-in-class (islet 1 and PAX6 for pancreas and OTP for lung) NET-specific markers are not on the test menus of most clinical laboratories [15,22–24]. Many laboratories have switched from polyclonal to better-performing (for adenocarcinoma applications) monoclonal PAX8 antibodies, the latter of which are non-reactive in pancreatic NETs (i.e., polyclonal PAX8-positivity in pNETs is due to cross-reactivity with PAX6). Even with access to all the best-performing markers at the University of Iowa, up to 5% of NETs still defy site-of-origin assignment after exhaustive immunohistochemical and radiologic evaluation. Against this backdrop, the lead authors of the 2022 World Health Organization NET Classification stated that there remains a critical need for additional biomarkers to better classify NETs [25].

Copy-number alterations (CNAs) are changes in chromosomal content that result in gain or loss of. copies of DNA segments, while functional copy-number alterations (fCNAs) are changes in chromosomal content that also impact expression of genes within the region. Somatic fCNAs are predicted to be cancer drivers as opposed to bystander lesions [26]. CNAs can be detected through techniques such as whole-genome sequencing (WGS), optical genome mapping, chromosomal microarray platforms (CMA) or fluorescence in situ hybridization (FISH), while fCNAs can be detected through pairing those techniques with gene-expression analysis. Over the last decade, CNA-profile studies of NETs have yielded promising results, but notable discrepancies between studies have been observed [27–37]. Robust analysis of CNA profile differences between pNETs and sbNETs is still needed.

We present here the results of a pipeline used to identify differences in fCNA profiles between pNETs and sbNETs, as well as between early- and late-disease-progression tumors, with the goal of developing a panel of clinically applicable FISH probes for use in diagnostic and prognostic NET biomarker testing. This type of testing has direct relevance to metastatic NETs of unknown origin detected in the liver. To identify diagnostic NET biomarkers, a discovery cohort of patient-matched normal primary metastatic tumors underwent CMA and RNA-sequencing to identify fCNAs in 64 patients diagnosed with GEP NET (31 pNETs and 33 sbNETs). We further analyzed the prognostic value of these fCNAs in NETs, specifically with regard to time to progression. We replicated fCNAs using FISH on patient-specimen-derived tissue microarrays (TMAs) and selected probes based on their location within fCNAs of interest. Based on these collective findings, we propose a testing algorithm for primary site (pNET vs sbNET) and disease progression (late disease progression [LDP] or early disease progression [EDP]) that can be rapidly and inexpensively performed on formalin-fixed, paraffin-embedded (FFPE) NET tissue. Overall, these findings support fCNAs' utility as effective diagnostic and prognostic biomarkers in NETs.

2. Results

2.1. Differences in Copy-Number Alteration between pNETs and sbNETs

To establish primary and metastatic CNA profiles in pNETs and sbNETs, normal primary metastatic tumors underwent CMA profiling. In total, 47 pNET (28 primary, 19 metastatic) and 63 sbNET (32 primary, 31 metastatic) specimens were assessed by CMA. No significant CNA differences were observed between primary and metastatic tumors for either NET type (Supplementary Figure S1 and S2).

Considerable evidence suggests there are unique CNAs in pNETs and sbNETs, but discrepancies between studies have been observed [27–32]. To determine the comprehensive CNA profiles of pNETs and sbNETs, normal-tissue–primary-tumor pairs underwent CMA profiling. A total of 49 pNET and 63 sbNET patients were tested. We observed more copy-number-gain events in chromosomes 4, 5, 7, 9, 12, 13, 14, and 17–20 in pNETs (Fisher exact test $p < 0.05$). Copy-number-loss events in chromosomes 9 and 18 were detected almost exclusively in sbNETs (Fisher's exact test $p < 0.05$). These observations indicate robust and reproducible CNA-profile differences between pancreatic and small-bowel NETs (Figure 1 and Supplementary Table S1).
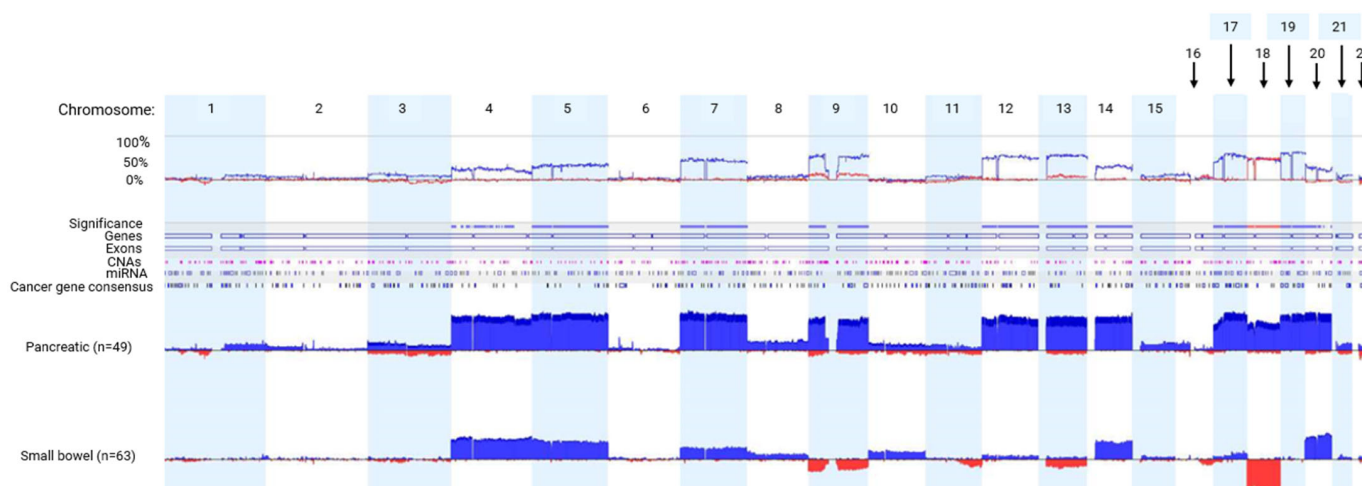
Figure 1. CMA data comparing pNET and sbNET tumor samples. The top row indicates chromosomes 1–22. Below is the frequency of the CNA events. Significance indicated by blue significance line. Genes, exons, CNAs, microRNAS (miRNAs), and cancer-related genes are listed below the significance bar. Blue represents copy-number gain. Red represents copy-number loss.

Functional copy-number alterations (fCNAs) are somatic changes in chromosomal content that affect the expression of genes within the region. To establish fCNA profiles in pNETs and sbNETs, we performed patient-matched RNA-sequencing of 31 pNETs (Supplementary Table S2) and 33 sbNETs (Supplementary Table S3) that underwent CMA profiling. To analyze the prognostic value of fCNAs in NETs, we separated our samples based on time to progression: late disease progression, or LDP, (>24 months until progression, n = 17) and early disease progression, or EDP, (<24 months until progression, n = 46). CNAs that were present in at least 15% of the cohort with significant concordant gene-expression changes (increased expression in a chromosomal gain and decreased expression in chromosomal loss) were identified as potential fCNA biomarkers (Table 1). fCNA profiles were compared, and a panel of differentiating fCNAs was selected (Table 2).

Table 1. fCNA loci and examples of genes within those loci that exhibited copy-number alterations and concordant gene-expression changes.

fCNA Locus & *Genes*	*p*	FDR	CNA (%)			RNA-Seq (Log2Fold)			
			L	N	G	L	N	G	Δ N vs L or G
4p16.3									
family with sequence similarity 218 (FAM218A)	6.04×10^{-6}	0.01	0%	48%	52%	NA	0.7	3.7	3.0
UNC-5 Netrin Receptor C (UNC5C)	0.0002	0.03	0%	42%	58%	NA	1.3	4.0	2.7
5q21.2-31.3									
CART Prepropeptide (CARTPT)	7.98×10^{-5}	0.03	0%	35%	65%	NA	0.6	6.4	5.8
Protocadherin Gamma Subfamily B, 3 (PCDHGB3)	0.0002	0.03	0%	42%	58%	NA	0.6	3.1	2.5
7q21.3-q31.1									
ATP-Binding Cassette Subfamily B MemberB (ABCB1)	0.0004	0.04	0%	39%	61%	NA	1.6	5.2	3.6
Reelin (RELN)	0.0004	0.04	0%	35%	65%	NA	0.8	4.7	3.9
9p24.2-q34.11									
Very-Low-Density Lipoprotein Receptor (VLDLR)	0.0001	0.03	3%	42%	55%	−0.1	−0.4	1.3	1.6
Torsin Family 1 Member B (TOR1B)	0.0004	0.04	3%	39%	58%	0.6	0.8	1.7	0.9
17p11.2-13.1 17q11.2–15.3									
TNF Receptor-Associated Factor 4 (TRAF4)	0.0001	0.03	3%	26%	71%	−0.2	−0.4	1.3	1.7
Ras-Related Dexamethasone Induced 1 (RASD1)	0.0003	0.03	6%	42%	52%	4.5	1.1	4.5	3.0
18q21.1									
Ectopic P Granules 5 Autophagy Tethering Factor (EPG5)	0.0002	0.01	64%	36%	0%	−0.6	0.2	NA	−0.9
Ferrochelatase (FECH)	0.001	0.03	64%	36%	0%	−0.3	0.3	NA	−0.6
19q13.12-13.42									
RNA Polymerase II Subunit I (POLR2I)	0.0001	0.03	0%	32%	68%	NA	1.0	3.1	2.0
Leucine-Rich Repeat and Fibronectin Type III Domain Containing 1 (LRFN1)	7.27×10^{-5}	0.03	0%	32%	68%	NA	−0.7	1.6	2.3

L = loss. N = normal. G = gain. Δ = difference. *p*-value, false discovery rate (FDR).

Table 2. Differential panel of CNAs and associated commercially available and clinically used cancer-related gene probes.

fCNA Results	Biomarker	Commercially Available and Clinically Used Probes (Locus)
1q21.3+	EDP	*CKS1B* (1q21.3)
4p16.3+	LDP	*FGFR3* (4p16.3)
5q31.2-31.3+	EDP	*CSF1R* (5q32)
7q21.3-q31.1+	pNET/EDP	*MET* (7q31.2)
9p24.2-q34.11+	pNET	*CDKN2A* (9p21.3)

Table 2. *Cont.*

fCNA Results	Biomarker	Commercially Available and Clinically Used Probes (Locus)
17p11.2-17q13.1+	pNET	*ERBB2* (17q12)
17q11.2-17q15.3+	EDP	
18q21.1-	sbNET	*SMAD4* (18q21.2)
19q13.12-19q13.42+	pNET	*CCNE1* (19q12)

EDP = early disease progression. LDP = late disease progression. + indicates copy-number gain. - indicates copy-number loss.

The results showed that gains in 5q31, 7q31.1, 9p22.1, 17q11.2, 18q21.1, and 19q13.2 indicated a pancreatic primary tumor site, while a gain in 4p16.3 and a loss in 9p22.1 and/or 18q21.1 indicated a small-bowel primary site. Notable loss of chromosome 18 in sbNETs is well established in the literature [27,29,30,33–36]. Potential prognostic NET biomarkers included gains in 7q31.1, 9p22.1, and 19q13.2.

2.2. FISH Validation of fCNA Differences between pNETs and sbNETs

2.2.1. Diagnosis

FISH is a cytogenetic technique that can be performed on formalin-fixed, paraffin-embedded (FFPE) tissue to identify gene- and locus-specific CNAs. To replicate the evidence of the diagnostic potential of our selected fCNAs and respective probes, FISH analyses were performed on 300 nuclei of pNET (n = 60, Supplementary Table S4) and sbNET (n = 82, Supplementary Table S5) FFPE specimens. Our results indicate that CCNE1 copy-number gain is the strongest indicator of the primary site, with observed 5x higher rates in pNET samples (44% vs. 9%, X^2 = 31.87, *p* < 0.00001) (Table 3). Additional copy-number gains in SMAD4 (25% vs. 5%, X^2 = 15.69, *p* = 0.00008), ERBB2 (22% vs. 6%, X^2 = 10.63, *p* = 0.001), and CDKN2A (22% vs. 7%, X^2 = 9.07, *p* = 0.003) were observed 3–5× more frequently in pNETs tumors (Figure 2). Copy-number loss in SMAD4 was reported in 60% of sbNET tumors, which is consistent with the literature [27,29,30,33–36]. Normal copy-number status in CCNE1 was significantly more frequent in sbNET tumors (64% vs. 40%, X^2 = 10.99, *p* = 0.0009). There were no significant CNA differences between pNET and sbNET tumors reported in CKS1B, FGFR3, CSF1R, and MET.

Table 3. FISH results assessing the average percentage of copy-number loss, normal copy-number status, and gain of biomarkers between pNETs and sbNETs. X^2 = Chi-square.

Probe	CN Loss (%)	CN Normal (%)	CN Gain (%)
CKS1B		X^2 = 2.59 *p*-value (*p*) = 0.27	
pNET (n = 27)	36	54	9
sbNET (n = 26)	27	59	14
X^2	1.88	0.4	1.17
p	0.17	0.53	0.28
FGFR3		X^2 = 7.04 *p* = 0.70	
pNET (n = 16)	26	51	23
sbNET (n = 44)	21	55	24
X^2	0.7	0.32	0.03
p	0.4	0.57	0.87

Table 3. *Cont.*

Probe	CN Loss (%)	CN Normal (%)	CN Gain (%)
CSF1R		$X^2 = 4.63\ p = 0.10$	
pNET (n = 21)	17	56	27
sbNET (n = 31)	23	62	15
X^2	1.13	0.74	4.34
p	0.29	0.39	0.04
MET		$X^2 = 5.84\ p = 0.054$	
pNET (n = 42)	24	53	24
sbNET (n = 53)	28	62	11
X^2	0.42	1.64	5.84
p	0.52	0.2	0.02
CDKN2A		$X^2 = 9.25\ p = 0.01$	
pNET (n = 19)	22	56	22
sbNET (n = 14)	29	64	7
X^2	1.29	1.33	9.07
p	0.26	0.25	0.003
ERBB2		$X^2 = 10.77\ p = 0.005$	
pNET (n = 37)	22	56	22
sbNET (n = 31)	29	65	6
X^2	1.29	1.69	10.63
p	0.26	0.19	0.001
SMAD4		$X^2 = 29.12\ p < 0.00001$	
pNET (n = 22)	26	49	25
sbNET (n = 17)	60	35	5
X^2	23.58	4.02	15.69
p	<0.00001	0.04	0.00008
CCNE1		$X^2 = 21.92\ p\ 0.00001$	
pNET (n = 22)	16	40	44
sbNET (n = 17)	28	64	9
X^2	4.04	10.99	31.87
p	0.04	0.0009	<0.00001

CN = copy number. *p*-value calculated by Chi-square test (X^2). False discovery rate (FDR) = 0.006.

Thresholding copy-number loss on FISH of FFPE sections is challenging, as signal is assessed in a 2D section of a 3D structure (i.e., the nucleus), resulting in the incorrect impression of loss in some subsets of normal nuclei. We assessed the background apparent deletion rate due to sectioning and found an average background deletion rate of 28.3%. We used this important value to distinguish between loss due to artifact and true copy-number loss (Supplementary Table S6).
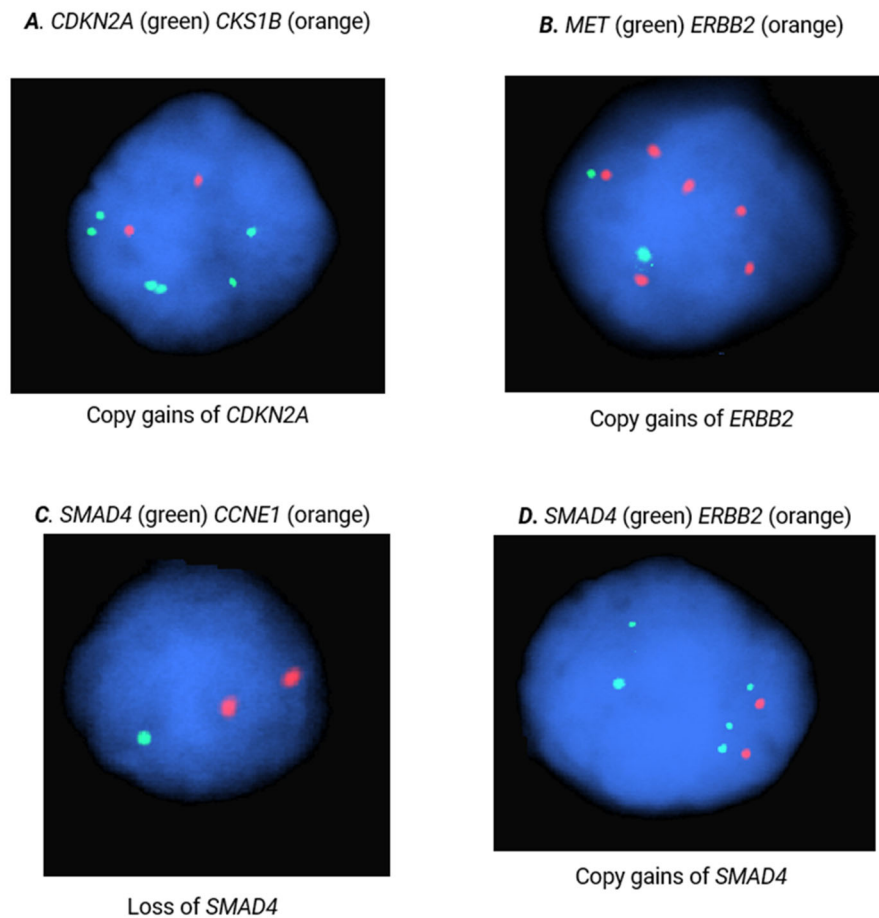
Figure 2. FISH analysis of CKS1B, MET, CDKN2A, ERBB2, SMAD4, and CCNE1. Images are representative of copy gains of (**A**) CDKN2A, (**B**) ERBB2, and (**C**) SMAD4, as well as loss of (**D**) SMAD4.

2.2.2. Prognosis

Next, we assessed whether these same fCNAs could be used as prognostic NET biomarkers. To determine if our fCNAs findings could predict disease progression, we separated our specimens into late-disease-progression (LDP) and early-disease-progression (EDP) samples with a cutoff of 5.5 years until reported disease progression. FISH analyses were performed on 300 nuclei of pNET (LDP = 24, EDP = 17) and sbNET (LDP = 41, EDP = 36) FFPE specimens. Copy-number gain in CDKN2A was 2.2× more frequent in LDP pNET tumors (42% vs. 19%, X^2 = 12.48, *p* = 0.0004) (Table 4). SMAD4 copy-number gain was 2.9× more frequent in EDP pNET tumors (42% vs. 10%, X^2 = 11.50, *p* = 0.0007). There were no prognostic implications for sbNET samples using these probes in our data set (Supplementary Table S7). These results validate the use of CNAs in CDKN2A and SMAD4 as independent potential prognostic pNET biomarkers.

Table 4. FISH results assessing the average percentage of copy-number loss, normal copy-number status, and gain of biomarkers between LDP and EDP.

Probe	CN Loss (%)	CN Normal (%)	CN Gain (%)
CKS1B		X^2 = 1.81 *p* = 0.41	
LDP (n = 6)	36	58	7
EDP (n = 10)	44	48	8
X^2	1.45	1.79	0.08
p	0.23	0.18	0.77

Table 4. *Cont.*

Probe	CN Loss (%)	CN Normal (%)	CN Gain (%)
FGFR3		$X^2 = 36.55\ p < 0.00001$	
LDP (n = 15)	24	52	24
EDP (n = 1)	63	32	4
X^2	31.76	7.9	16.39
p	0.00001	0.005	0.00005
CSF1R		$X^2 = 1.41\ p = 0.49$	
LDP (n = 13)	19	56	24
EDP (n = 6)	13	61	26
X^2	1.41	0.4	0.08
p	0.23	0.53	0.78
MET		$X^2 = 0.09\ p = 0.96$	
LDP (n = 16)	24	49	27
EDP (n = 11)	23	52	27
X^2	0.06	0.08	0.01
p	0.81	0.78	0.93
CDKN2A		$X^2 = 12.49\ p = 0.002$	
LDP (n = 6)	16	42	42
EDP (n = 3)	23	58	19
X^2	1.56	5.12	12.48
p	0.21	0.02	0.0004
ERBB2		$X^2 = 2.80\ p = 0.25$	
LDP (n = 15)	20	52	28
EDP (n = 10)	27	54	19
X^2	1.36	0.08	2.25
p	0.24	0.78	0.13
SMAD4		$X^2 = 12.78\ p = 0.002$	
LDP (n = 5)	37	53	10
EDP (n = 14)	23	48	29
X^2	4.67	3.02	11.5
p	0.03	0.08	0.0007
CCNE1		$X^2 = 0.52\ p = 0.77$	
LDP (n = 5)	15	39	46
EDP (n = 14)	17	42	41
X^2	0.15	0.19	0.51
p	0.7	0.67	0.48

CN = copy number. LDP = late disease progression. EDP = early disease progression. *p*-value calculated by Chi-square test (X^2). False discovery rate (FDR) = 0.006.

2.3. Logistic Regression, Performance Metrics and Clinical Decision Tree Development

Logistic regression analysis is used to determine the probability of multiple independent variables with one dichotomous outcome. Logistic regression can be used to analyze the sensitivity, specificity, and receiver operating characteristic curve (ROC) metrics to assess the quality of a model. Using our FISH data set, each specimen per probe was given a

"normalized score" (see Clinical Decision Tree Development in the Methods section) to use for logistic regression analysis (Supplementary Table S8). The results indicate MET, ERBB2, SMAD4, and CCNE1 copy-number status is significantly associated with primary tumor site (Table 5). CCNE1 had the strongest effect on primary site (0.92–1.00, CI = 0.41–1.00, p = 0.034), followed by SMAD4 (0.90–1.00, CI = 0.39–1.00, p = 0.046), ERBB2 (0.62–0.99, CI = 0.43–0.99, p = 0.001), and MET (0.70–0.93, CI = 0.33–0.99, p = 0.035). CDKN2A had a higher effect than MET on primary site, however, it did not reach significance in multivariate analysis. The performance metrics of our model are comparable to those achieved with IHC (Table 5) [14–16]. Based on these metrics, our model resulted in an area under the ROC curve (AUC) score of 0.902 (Figure 3).

Table 5. Logistic regression results based on primary tumor site. (a) Reported scores of statistical analyses per probe. (**b**) Quality control metrics for the overall model with reported AUC.

(a.) Probe	Score	Effect Size	95% CI	z Value	*p*-Value
CKS1B	−40 to −10	0.72–0.88	0.07–1.00	−1.19	0.232
FGFR3	−30–2	0.59–0.74	0.15–0.98	−1.25	0.212
CSF1R	90	0.70	0.30–0.92	1.91	0.056
MET	80	0.70	0.33–0.91	2.11	0.035
CDKN2A	70–80	0.77–0.88	0.23–1.00	1.61	0.107
ERBB2	60–80	0.62–0.95	0.43–0.99	3.45	0.001
SMAD4	50–90	0.90–1.00	0.39–1.00	2.00	0.046
(b.) Performance Metrics					
PseudoR2			0.44		
p-value			5.23×10^{-15}		
Sensitivity			0.68		
Specificity			0.89		
AUC			0.902		

CI = confidence interval. AUC = area under the ROC curve.

When assessing the prognostic impact of these probes, gain of CCNE1 was associated with early disease progression (EDP) in pNETs (gain, 0.46–0.89, CI = 0.24–0.99, p = 0.039) and sbNETs (normal, 0.58–0.91, CI = 0.41–0.99, p = 0.043) (Supplementary Table S9). In addition, FGFR3 gain was associated with EDP in sbNETs (0.70–0.95, CI = 0.52–0.99, p = 0.0004) (Supplementary Table S10). CSF1R loss was suggestive of LDP in sbNETs (0.57, CI = 0.40–0.73, p = 0.07). Unlike our single-probe analysis, CDKN2A and SMAD4 had no impact on pNET prognosis in the multivariate analysis.

We created a clinical decision tree (DT) using CNAs as diagnostic biomarkers (Figure 4). Our DT suggests assessing copy-number status for ERBB2, CCNE1, CDKN2A, and MET is effective for differentiating between pNETs and sbNETs. If ERBB2 is gained, the tumor has a 90% chance of being from the pancreas; however, if ERBB2 is lost or normal CCNE1 copy-number status should be assessed. If CCNE1 is gained, then the tumor has a greater than 80% chance of being from the pancreas but if it is lost or normal, CDKN2A copy-number status should be assessed. If CDKN2A is gained or normal, the tumor has a slightly greater than 60% chance of being from the pancreas and a 40% chance of being from the small bowel. If CDKN2A is lost and MET is either lost or normal, the sample has a greater than 80% chance of being from the small bowel; however, if MET is gained and ERBB2 is normal, it has a greater than 85% chance of being from the pancreas. Lastly, if MET is gained but ERBB2 is lost, the tumor has a greater than 90% chance of being from the small bowel. SMAD4 was not differential in our DT, which may be due to CCNE1 and SMAD4 copy number being highly correlated in our dataset (0.635) (Supplementary Table S11). Overall,

these findings support the use of CNAs in MET, CDKN2A, ERBB2, and CCNE1 as simple diagnostic NET biomarkers.
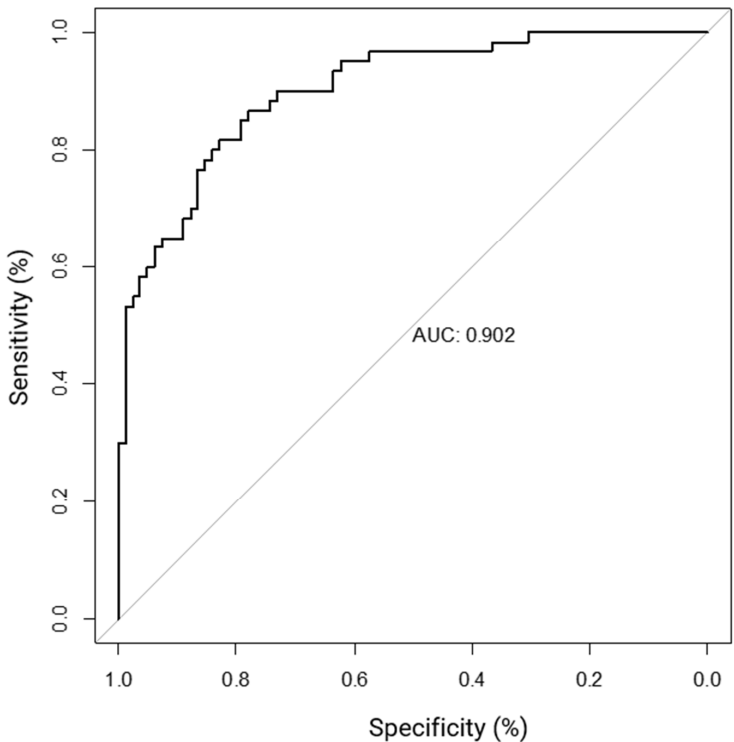
Figure 3. Receiver operating characteristic curve (ROC) curve analysis using CNAs in CCNE1, SMAD4, ERBB2, and CDKN2A as diagnostic NET biomarkers.
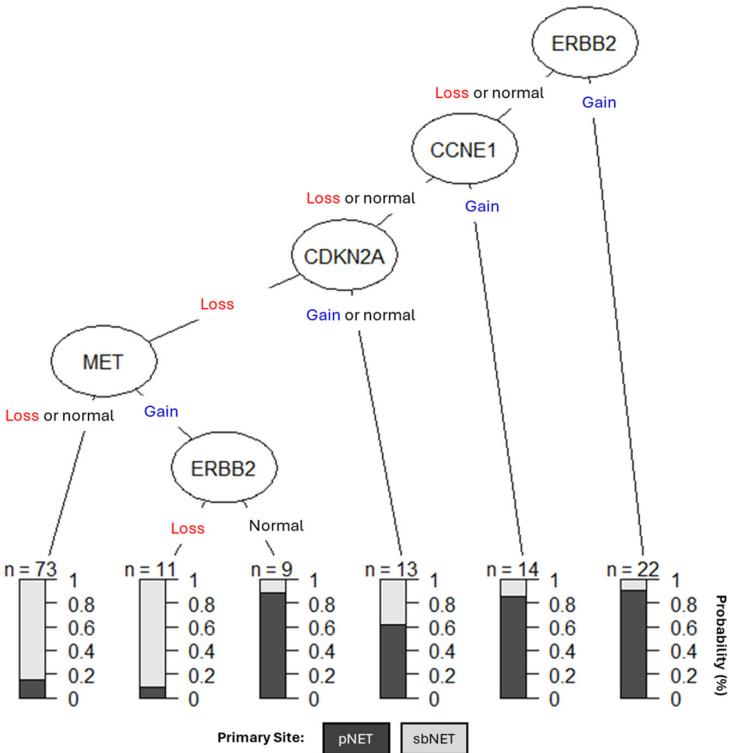
Figure 4. Clinical DT models using CNAs in ERBB2, CCNE1, CDKN2A, and MET as NET biomarkers. The shading of the boxes represents the most likely primary tumor site, while the numbers on the right-hand side represent the predicted probabilities by site.

3. Discussion

The aim of this paper was to determine if CNAs could be used as NET biomarkers by integrating patient-matched CNA and gene-expression data to identify fCNAs. We replicated fCNAs by selecting probes based on their location within fCNAs of interest using FISH on patient-specimen-derived tissue microarrays with the goal of developing a fast clinical DT that could be applied in any testing laboratory to expedite medical decision-making.

FISH is a widely available methodology that offers a cost-effective approach with relatively rapid turnaround time. Through the identification, replication, and prioritization of FISH probes in this study, there is potential to improve the diagnostic assessment of NETs while reducing the cost and the processing time of results, thus improving patient care.

Our findings support the use of CNAs in *MET*, *ERBB2*, *SMAD4*, and *CCNE1* as diagnostic NET biomarkers and resulted in an AUC of 0.902. This compares favorably to a previously published immunochemistry-based algorithm that resulted in an ROC of 0.864 for distinguishing between tumors of pancreatic versus small-bowel or pulmonary origin [38]. As previously mentioned, IHC is currently used to infer site of origin in metastatic NETs of occult origin [14–16]. Taking the evidence together, we recommend assessing the copy-number status of *MET*, *CDKN2A*, *ERBB2*, and *CCNE1* to differentiate between pNETs and sbNETs. Although *SMAD4* was statistically associated with primary site, its copy-number status was highly correlated with that of *CCNE1* (0.635). The current leading NET prognostic biomarkers include tumor grade, tumor stage, and IHC analysis of genes such as p53 and ATRX/DAXX [15,23,25]. Our findings suggest that *FGFR3*, *CDKN2A*, *SMAD4*, and *CCNE1* are valuable prognostic NET biomarkers. Many studies of other tumor types show that *CCNE1* gain is a key marker of poor prognosis that may dictate more aggressive clinical management [39–45].

Limitations of our study include the moderate sample size of the dataset. This reflects the rarity of NETs, a factor that makes it challenging to gather larger cohorts, and this is especially limiting for our time-to-progression analysis. For our CMA discovery cohort, the average PFS was 2.4 years, which is different from the PFS of our FISH validation cohort and that in the literature, which is approximately 5.5 years [27–30,33]. Another limitation includes the missing values of the dataset. To combat this, we used the median score for each probe to impute the missing data; however, observed FISH results for all variables and all samples would provide more accurate overall results. A general limitation is that data gathered from clinical samples and electronic health records are not always complete across all samples.

To our surprise, there were no significant CNA differences in *FGFR3* and *CSF1R* between pNETs and sbNETs using FISH and logistic regression analyses even though we observed significant CNA differences in our CMA-data discovery cohort. Secondly, *CKS1B* copy-number gain was not associated with PFS in this study but has been correlated with poor PFS in pan-cancer analyses [46–52]. It is important to note that those studies did not include assessments of the correlation between GEP NET prognosis and *CKS1B* copy-number status. Lastly, we determined there was no significant difference in *CDKN2A* copy-number loss between pNETs and sbNETs, although our CMA data suggested otherwise. *CDKN2A* has been shown to be a tumor suppressor in pNETs, and focal *CDKN2A* loss has been observed [28]. Additionally, *CDKN2A* loss might not have been observed due to the inherent challenges of assessing loss (as opposed to gain) in FFPE samples.

In summary, we found significant CNA differences in *CDKN2A*, *ERBB2*, *SMAD4*, and *CCNE1* between pNET and sbNET tumor samples after combined analyses of chromosomal microarrays, RNA sequencing, and fluorescence in situ hybridization data. Using the FISH data, we performed logistic regression analysis and derived performance metrics while developing a clinical decision tree to help determine the primary tumor site and guide risk-stratified therapeutic decisions for metastatic tumors of unknown origin detected in the liver. This combinatorial approach to biomarker identification has proven highly effective

and may represent a powerful way to define clinically relevant biomarkers for additional NET primary sites in the future.

4. Materials and Methods

4.1. Patient Cohort

All patients in this single-institution study were enrolled under an Institutional Review Board-approved protocol. The CMA discovery cohort consisted of patient-matched normal primary metastatic tumors of 47 pNETs (28 primary, 19 metastatic) and 63 sbNETs (32 primary, 31 metastatic) (Supplementary Figure S3). Normal primary metastatic tumors include the primary and metastatic tumor specimens as well as normal, healthy adjacent tissue derived from the same patient. The FISH replication cohort consisted of patient-matched normal primary metastatic tumors of 84 pNETs (76 primary, 3 metastatic liver, 5 metastatic lymph node) and 98 sbNETs (86 primary, 7 metastatic liver, 5 metastatic lymph node). Patient-cohort demographic data are listed in Supplementary Table S12. Fresh tissue samples were collected and placed in RNAlater solution (Thermo Fisher Scientific, Waltham, MA, USA), and nucleic acids were isolated using the RNeasy Plus Universal Mini Kit (Qiagen, Valencia, CA, USA) or DNeasy blood & Tissue Kit (Qiagen, Valencia, CA, USA) per the protocols recommended by the manufacturers.

4.2. Microarray Protocols

Microarray experiments were performed using the NimbleGen Human CGH 720 K Whole-Genome Tiling version 3.0 array (Roche NimbleGen; Madison, WI, USA) and the Affymetrix CytoScan High-Definition (HD) array (Affymetrix array, Santa Clara, CA, USA) according to the manufacturers' instructions. Calculation of log2 ratio values and quality-control metrics were assessed using the NimbleScan software tool (version 2.5; Roche NimbleGen) or the ChAS (Chromosome Analysis Software) tool (version 1.1.2; Affymetrix) (CytoScan). CNA calling and data interpretation were performed using the Nexus Copy Number software (version 6.1, BioDiscovery; El Segundo, CA, USA) and the rank segmentation algorithm (for Nimblegen arrays) or the SNPRank segmentation algorithm (CytoScanHD) supplied with the Nexus software suite (version 2.5; Roche NimbleGen) [53]. Allele-specific copy-number analysis of tumors (ASCAT) was performed to identify ploidy and percent normal tissue.

4.3. RNA Processing

RNA-seq was performed within the Genomics Division of the University of Iowa Institute of Human Genetics (University of Iowa, Iowa City, IA, USA) using the Illumina TruSeq protocol (Illumina, Inc., San Diego, CA, USA), as previously described [54]. RNA-seq count data were normalized using FPKM. To identify differentially expressed genes, TopHat (v 2.1.0, John Hopkins University, Baltimore, MA, USA), Cuffquant, Cuffnorm, and Cuffduff were performed, comparing tumors to healthy adjacent pancreatic or small-bowel tissue. Statistically significant expression change was determined by assessing the false discovery rate (FDR) adjusted *p*-value (q-value), with significance defined as q < 0.05.

4.4. fCNA Identification

The R package (v 3.4.4) iGC [55] integrates sample-paired copy-number and gene-expression analysis to identify concordant differential gene expression. Log2 copy-number values from NimbleGen (Roche NimbleGen; Madison, WI, USA) or Affymetrix (Affymetrix array, Santa Clara, CA, USA) were utilized to analyze the association between copy number and mRNA levels of 31 pNET and 33 sbNET samples. CNAs that were observed in at least 20% of samples were assessed. Allelic-imbalance and loss-of-heterozygosity lesions were removed. Genes for which expression was predicted to be driven by either copy-number gain (and increased expression) or copy-number loss (and decreased expression) events and which met previously defined *p* and FDR thresholds were retained. No fold-change threshold was utilized for the iGC analysis.

4.5. Fluorescence In Situ Hybridization (FISH)

TMAs were assembled from formalin-fixed, paraffin-embedded lesions of 60 pNET and 82 sbNET primary and metastatic specimens arrayed in triplicate (2-micron sections). FISH studies were performed using Empire Genomics FISH probes *CKS1B*-20-OR, *FGFR3*-20-OR, *CSFR1*-20-GR, *MET*-20-GR, *CDKN2A*-20-GR, *ERBB2*-20-OR, *SMAD4*-20-GR, and *CCNE1*-20-OR (Empire Genomics, Inc., New York, NY, USA) per the protocol recommended by the manufacturer (empiregenomics.com/resources/protocols-procedures). One hundred nuclei per section and three sections per patient specimen, for a total of three hundred nuclei, were scored. Briefly, slides were baked for a minimum of 8 h at 45 °C, deparaffinized with Hemo-De, and then rehydrated before they were heated in Dako pre-treatment 20×. The samples were digested with pepsin at 37 °C for 5 min. After digestion, slides were washed with Dako buffer and dehydrated with a series of 70%, 85%, and 100% ethanol. The slides were then probed, denatured, and hybridized for 48 h at 37 °C. Unbound probe was washed from the slides, and they were counterstained with DAPI. FISH slides were analyzed at 100× magnification using CytoVision (Leica Microsystems, Wetzlar, Germany) filters.

Counts for loss-, normal-, and gain-signal-pattern nuclei were average for each specimen and probe set. Statistical differences were assessed using the Chi-Square test with significance defined as $p < 0.05$. Firth's bias-reduced logistic regression was used to estimate the predicted probability of association of CNAs with a given tissue of origin. Copy-number loss was defined as occurrence observed in a proportion less than or equal to 28.3% of nuclei showing fewer than two copies to account for "pseudo-loss" due to the plane of sectioning. Copy-number gain was defined as occurrence observed in a proportion greater than or equal to 15.3% of nuclei. These values were calculated by assessing the average percent copy-number loss, normal copy-number status, and copy-number gain within our entire dataset and selecting the greatest-variable-range value for pNETs (loss) and sbNETs (gain), respectively. Duplicate CNAs of the same probe set with the largest variable ranges were chosen. Samples outside of these loss and gain thresholds were determined to be normal. Descriptive statistics for copy-number loss, normal copy-number status, and copy-number gain are listed in the table provided (Supplementary Table S13).

4.6. Logistic Regression Analysis and DT Development

Logistic regression and statistical analyses were performed by assessing the 8 biomarker-locus variables in the FISH dataset. To do so, each biomarker in each sample was given a score. The score was determined by calculating the percent normal nuclei, subtracting the percent loss nuclei, and adding the percent gain nuclei. Therefore, a sample probed with a biomarker that resulted in 60% normal, 28% loss, and 12% gain nuclei would be given a score of 44 ($60 - 28 + 12$). Loss, normal, and gain values were determined by thresholds set based on the original variables. Missing data were imputed with the median score for each probe. The biomarker and response variables were tested within a pipeline with the Analysis of Overdispersed Data (aod- version 1.3.2) and ggplot2 (version 3.4.4) R (v 4.3.1) packages.

DT dataset curation was performed by assessing the 8 biomarker-locus variables in the FISH dataset categorically. For example, if a probe for any given sample was lost, a value of 1 was designated, while normal and gains were assigned values of 2 and 3, respectively. Missing data points were assigned a value of 0. The decision tree was developed using the rpart (version 4.1.23) and partykit (version 1.2.20) R (v 4.3.1) packages.

Institutional Review Board Statement: The study was conducted in accordance with the Declaration of Helsinki. Patients presenting to the University of Iowa with pNETs and sbNETs were consented for genetic studies and entered into a tumor registry approved by the University of Iowa Institutional Review Board (IRB#: 199911057).

Informed Consent Statement: Informed written consent was provided by all patients in accordance with a protocol approved by the University of Iowa Institutional Review Board (IRB Number 199911057), and studies were conducted in accordance with the Belmont Report.

Data Availability Statement: Data are contained within the article and Supplementary Materials.

Conflicts of Interest: The authors declare no conflicts of interest.

References

1. Wang, S.C.; Parekh, J.R.; Zuraek, M.B.; Venook, A.P.; Bergsland, E.K.; Warren, R.S.; Nakakura, E.K. Identification of unknown primary tumors in patients with neuroendocrine liver metastases. *Arch. Surg.* **2010**, *145*, 276–280. [CrossRef] [PubMed]
2. Modlin, I.M.; Oberg, K.; Chung, D.C.; Jensen, R.T.; de Herder, W.W.; Thakker, R.V.; Caplin, M.; Delle Fave, G.; Kaltsas, G.A.; Krenning, E.P.; et al. Gastroenteropancreatic neuroendocrine tumours. *Lancet Oncol.* **2008**, *9*, 61–72. [CrossRef] [PubMed]
3. Dasari, A.; Shen, C.; Halperin, D.; Zhao, B.; Zhou, S.; Xu, Y.; Shih, T.; Yao, J.C. Trends in the Incidence, Prevalence, and Survival Outcomes in Patients With Neuroendocrine Tumors in the United States. *JAMA Oncol.* **2017**, *3*, 1335–1342. [CrossRef] [PubMed]
4. Caplin, M.E.; Pavel, M.; Ruszniewski, P. Lanreotide in metastatic enteropancreatic neuroendocrine tumors. *N. Engl. J. Med.* **2014**, *371*, 1556–1557. [CrossRef] [PubMed]
5. Rinke, A.; Muller, H.H.; Schade-Brittinger, C.; Klose, K.J.; Barth, P.; Wied, M.; Mayer, C.; Aminossadati, B.; Pape, U.F.; Blaker, M.; et al. Placebo-controlled, double-blind, prospective, randomized study on the effect of octreotide LAR in the control of tumor growth in patients with metastatic neuroendocrine midgut tumors: A report from the PROMID Study Group. *J. Clin. Oncol.* **2009**, *27*, 4656–4663. [CrossRef] [PubMed]
6. Brabander, T.; van der Zwan, W.A.; Teunissen, J.J.M.; Kam, B.L.R.; Feelders, R.A.; de Herder, W.W.; van Eijck, C.H.J.; Franssen, G.J.H.; Krenning, E.P.; Kwekkeboom, D.J. Long-Term Efficacy, Survival, and Safety of [(177)Lu-DOTA(0),Tyr(3)]octreotate in Patients with Gastroenteropancreatic and Bronchial Neuroendocrine Tumors. *Clin. Cancer Res.* **2017**, *23*, 4617–4624. [CrossRef] [PubMed]
7. Yao, J.C.; Phan, A.T.; Chang, D.Z.; Wolff, R.A.; Hess, K.; Gupta, S.; Jacobs, C.; Mares, J.E.; Landgraf, A.N.; Rashid, A.; et al. Efficacy of RAD001 (everolimus) and octreotide LAR in advanced low- to intermediate-grade neuroendocrine tumors: Results of a phase II study. *J. Clin. Oncol.* **2008**, *26*, 4311–4318. [CrossRef] [PubMed]
8. Yao, J.C.; Shah, M.H.; Ito, T.; Bohas, C.L.; Wolin, E.M.; Van Cutsem, E.; Hobday, T.J.; Okusaka, T.; Capdevila, J.; de Vries, E.G.; et al. Everolimus for advanced pancreatic neuroendocrine tumors. *N. Engl. J. Med.* **2011**, *364*, 514–523. [CrossRef] [PubMed]
9. Yao, J.C.; Fazio, N.; Singh, S.; Buzzoni, R.; Carnaghi, C.; Wolin, E.; Tomasek, J.; Raderer, M.; Lahner, H.; Voi, M.; et al. Everolimus for the treatment of advanced, non-functional neuroendocrine tumours of the lung or gastrointestinal tract (RADIANT-4): A randomised, placebo-controlled, phase 3 study. *Lancet* **2016**, *387*, 968–977. [CrossRef]
10. Raymond, E.; Dahan, L.; Raoul, J.L.; Bang, Y.J.; Borbath, I.; Lombard-Bohas, C.; Valle, J.; Metrakos, P.; Smith, D.; Vinik, A.; et al. Sunitinib malate for the treatment of pancreatic neuroendocrine tumors. *N. Engl. J. Med.* **2011**, *364*, 501–513. [CrossRef]
11. Kunz, P.L.; Graham, N.T.; Catalano, P.J.; Nimeiri, H.S.; Fisher, G.A.; Longacre, T.A.; Suarez, C.J.; Martin, B.A.; Yao, J.C.; Kulke, M.H.; et al. Randomized Study of Temozolomide or Temozolomide and Capecitabine in Patients With Advanced Pancreatic Neuroendocrine Tumors (ECOG-ACRIN E2211). *J. Clin. Oncol.* **2023**, *41*, 1359–1369. [CrossRef] [PubMed]
12. Strosberg, J.R.; Fine, R.L.; Choi, J.; Nasir, A.; Coppola, D.; Chen, D.T.; Helm, J.; Kvols, L. First-line chemotherapy with capecitabine and temozolomide in patients with metastatic pancreatic endocrine carcinomas. *Cancer* **2011**, *117*, 268–275. [CrossRef] [PubMed]
13. Yao, J.C.; Voi, M.; Rouyrre, N.; Singh, S. Everolimus in ileum neuroendocrine tumours—Authors' reply. *Lancet* **2016**, *388*, 236–237. [CrossRef] [PubMed]
14. Bellizzi, A.M. Assigning site of origin in metastatic neuroendocrine neoplasms: A clinically significant application of diagnostic immunohistochemistry. *Adv. Anat. Pathol.* **2013**, *20*, 285–314. [CrossRef]
15. Bellizzi, A.M. Immunohistochemistry in the diagnosis and classification of neuroendocrine neoplasms: What can brown do for you? *Hum. Pathol.* **2020**, *96*, 8–33. [CrossRef] [PubMed]
16. Maxwell, J.E.; Sherman, S.K.; Stashek, K.M.; O'Dorisio, T.M.; Bellizzi, A.M.; Howe, J.R. A practical method to determine the site of unknown primary in metastatic neuroendocrine tumors. *Surgery* **2014**, *156*, 1359–1365; discussion 1356–1365. [CrossRef] [PubMed]
17. Erickson, L.A.; Papouchado, B.; Dimashkieh, H.; Zhang, S.; Nakamura, N.; Lloyd, R.V. Cdx2 as a marker for neuroendocrine tumors of unknown primary sites. *Endocr. Pathol.* **2004**, *15*, 247–252. [CrossRef] [PubMed]

18. Long, K.B.; Srivastava, A.; Hirsch, M.S.; Hornick, J.L. PAX8 Expression in well-differentiated pancreatic endocrine tumors: Correlation with clinicopathologic features and comparison with gastrointestinal and pulmonary carcinoid tumors. *Am. J. Surg. Pathol.* **2010**, *34*, 723–729. [CrossRef] [PubMed]

19. Folpe, A.L.; Gown, A.M.; Lamps, L.W.; Garcia, R.; Dail, D.H.; Zarbo, R.J.; Schmidt, R.A. Thyroid transcription factor-1: Immuno-histochemical evaluation in pulmonary neuroendocrine tumors. *Mod. Pathol.* **1999**, *12*, 5–8.

20. Bellizzi, A.M. SATB2 in neuroendocrine neoplasms: Strong expression is restricted to well-differentiated tumours of lower gastrointestinal tract origin and is most frequent in Merkel cell carcinoma among poorly differentiated carcinomas. *Histopathology* **2020**, *76*, 251–264. [CrossRef]

21. Bellizzi, A.M. An Algorithmic Immunohistochemical Approach to Define Tumor Type and Assign Site of Origin. *Adv. Anat. Pathol.* **2020**, *27*, 114–163. [CrossRef] [PubMed]

22. Schmitt, A.M.; Riniker, F.; Anlauf, M.; Schmid, S.; Soltermann, A.; Moch, H.; Heitz, P.U.; Kloppel, G.; Komminoth, P.; Perren, A. Islet 1 (Isl1) expression is a reliable marker for pancreatic endocrine tumors and their metastases. *Am. J. Surg. Pathol.* **2008**, *32*, 420–425. [CrossRef] [PubMed]

23. Graham, R.P.; Shrestha, B.; Caron, B.L.; Smyrk, T.C.; Grogg, K.L.; Lloyd, R.V.; Zhang, L. Islet-1 is a sensitive but not entirely specific marker for pancreatic neuroendocrine neoplasms and their metastases. *Am. J. Surg. Pathol.* **2013**, *37*, 399–405. [CrossRef]

24. Nonaka, D.; Papaxoinis, G.; Mansoor, W. Diagnostic Utility of Orthopedia Homeobox (OTP) in Pulmonary Carcinoid Tumors. *Am. J. Surg. Pathol.* **2016**, *40*, 738–744. [CrossRef] [PubMed]

25. Rindi, G.; Mete, O.; Uccella, S.; Basturk, O.; La Rosa, S.; Brosens, L.A.A.; Ezzat, S.; de Herder, W.W.; Klimstra, D.S.; Papotti, M.; et al. Overview of the 2022 WHO Classification of Neuroendocrine Neoplasms. *Endocr. Pathol.* **2022**, *33*, 115–154. [CrossRef] [PubMed]

26. Taylor, B.S.; Barretina, J.; Socci, N.D.; Decarolis, P.; Ladanyi, M.; Meyerson, M.; Singer, S.; Sander, C. Functional copy-number alterations in cancer. *PLoS ONE* **2008**, *3*, e3179. [CrossRef]

27. Andersson, E.; Sward, C.; Stenman, G.; Ahlman, H.; Nilsson, O. High-resolution genomic profiling reveals gain of chromosome 14 as a predictor of poor outcome in ileal carcinoids. *Endocr. Relat. Cancer* **2009**, *16*, 953–966. [CrossRef] [PubMed]

28. Scarpa, A.; Chang, D.K.; Nones, K.; Corbo, V.; Patch, A.M.; Bailey, P.; Lawlor, R.T.; Johns, A.L.; Miller, D.K.; Mafficini, A.; et al. Whole-genome landscape of pancreatic neuroendocrine tumours. *Nature* **2017**, *543*, 65–71. [CrossRef] [PubMed]

29. Banck, M.S.; Kanwar, R.; Kulkarni, A.A.; Boora, G.K.; Metge, F.; Kipp, B.R.; Zhang, L.; Thorland, E.C.; Minn, K.T.; Tentu, R.; et al. The genomic landscape of small intestine neuroendocrine tumors. *J. Clin. Investig.* **2013**, *123*, 2502–2508. [CrossRef]

30. Hashemi, J.; Fotouhi, O.; Sulaiman, L.; Kjellman, M.; Hoog, A.; Zedenius, J.; Larsson, C. Copy number alterations in small intestinal neuroendocrine tumors determined by array comparative genomic hybridization. *BMC Cancer* **2013**, *13*, 505. [CrossRef]

31. Hofving, T.; Arvidsson, Y.; Almobarak, B.; Inge, L.; Pfragner, R.; Persson, M.; Stenman, G.; Kristiansson, E.; Johanson, V.; Nilsson, O. The neuroendocrine phenotype, genomic profile and therapeutic sensitivity of GEPNET cell lines. *Endocr. Relat. Cancer* **2018**, *25*, X1–X2. [CrossRef] [PubMed]

32. Hu, W.; Feng, Z.; Modica, I.; Klimstra, D.S.; Song, L.; Allen, P.J.; Brennan, M.F.; Levine, A.J.; Tang, L.H. Gene Amplifications in Well-Differentiated Pancreatic Neuroendocrine Tumors Inactivate the p53 Pathway. *Genes. Cancer* **2010**, *1*, 360–368. [CrossRef] [PubMed]

33. Kulke, M.H.; Freed, E.; Chiang, D.Y.; Philips, J.; Zahrieh, D.; Glickman, J.N.; Shivdasani, R.A. High-resolution analysis of genetic alterations in small bowel carcinoid tumors reveals areas of recurrent amplification and loss. *Genes. Chromosomes Cancer* **2008**, *47*, 591–603. [CrossRef] [PubMed]

34. Kytola, S.; Hoog, A.; Nord, B.; Cedermark, B.; Frisk, T.; Larsson, C.; Kjellman, M. Comparative genomic hybridization identifies loss of 18q22-qter as an early and specific event in tumorigenesis of midgut carcinoids. *Am. J. Pathol.* **2001**, *158*, 1803–1808. [CrossRef] [PubMed]

35. Lollgen, R.M.; Hessman, O.; Szabo, E.; Westin, G.; Akerstrom, G. Chromosome 18 deletions are common events in classical midgut carcinoid tumors. *Int. J. Cancer* **2001**, *92*, 812–815. [CrossRef]

36. Simbolo, M.; Vicentini, C.; Mafficini, A.; Fassan, M.; Pedron, S.; Corbo, V.; Mastracci, L.; Rusev, B.; Pedrazzani, C.; Landoni, L.; et al. Mutational and copy number asset of primary sporadic neuroendocrine tumors of the small intestine. *Virchows Arch.* **2018**, *473*, 709–717. [CrossRef] [PubMed]

37. Gebauer, N.; Schmidt-Werthern, C.; Bernard, V.; Feller, A.C.; Keck, T.; Begum, N.; Rades, D.; Lehnert, H.; Brabant, G.; Thorns, C. Genomic landscape of pancreatic neuroendocrine tumors. *World J. Gastroenterol.* **2014**, *20*, 17498–17506. [CrossRef] [PubMed]

38. Koo, J.; Mertens, R.B.; Mirocha, J.M.; Wang, H.L.; Dhall, D. Value of Islet 1 and PAX8 in identifying metastatic neuroendocrine tumors of pancreatic origin. *Mod. Pathol.* **2012**, *25*, 893–901. [CrossRef] [PubMed]

39. Zhao, H.; Wang, J.; Zhang, Y.; Yuan, M.; Yang, S.; Li, L.; Yang, H. Prognostic Values of CCNE1 Amplification and Overexpression in Cancer Patients: A Systematic Review and Meta-analysis. *J. Cancer* **2018**, *9*, 2397–2407. [CrossRef]

40. Ayhan, A.; Kuhn, E.; Wu, R.C.; Ogawa, H.; Bahadirli-Talbott, A.; Mao, T.L.; Sugimura, H.; Shih, I.M.; Wang, T.L. CCNE1 copy-number gain and overexpression identify ovarian clear cell carcinoma with a poor prognosis. *Mod. Pathol.* **2017**, *30*, 297–303. [CrossRef]

41. Nakayama, N.; Nakayama, K.; Shamima, Y.; Ishikawa, M.; Katagiri, A.; Iida, K.; Miyazaki, K. Gene amplification CCNE1 is related to poor survival and potential therapeutic target in ovarian cancer. *Cancer* **2010**, *116*, 2621–2634. [CrossRef] [PubMed]

42. Nakayama, K.; Rahman, M.T.; Rahman, M.; Nakamura, K.; Ishikawa, M.; Katagiri, H.; Sato, E.; Ishibashi, T.; Iida, K.; Ishikawa, N.; et al. CCNE1 amplification is associated with aggressive potential in endometrioid endometrial carcinomas. *Int. J. Oncol.* **2016**, *48*, 506–516. [CrossRef] [PubMed]

43. Zhou, Z.; Bandla, S.; Ye, J.; Xia, Y.; Que, J.; Luketich, J.D.; Pennathur, A.; Peters, J.H.; Tan, D.; Godfrey, T.E. Cyclin E involved in early stage carcinogenesis of esophageal adenocarcinoma by SNP DNA microarray and immunohistochemical studies. *BMC Gastroenterol.* **2014**, *14*, 78. [CrossRef] [PubMed]

44. Farley, J.; Smith, L.M.; Darcy, K.M.; Sobel, E.; O'Connor, D.; Henderson, B.; Morrison, L.E.; Birrer, M.J.; Gynecologic Oncology, G. Cyclin E expression is a significant predictor of survival in advanced, suboptimally debulked ovarian epithelial cancers: A Gynecologic Oncology Group study. *Cancer Res.* **2003**, *63*, 1235–1241.

45. Matsushita, R.; Seki, N.; Chiyomaru, T.; Inoguchi, S.; Ishihara, T.; Goto, Y.; Nishikawa, R.; Mataki, H.; Tatarano, S.; Itesako, T.; et al. Tumour-suppressive microRNA-144-5p directly targets CCNE1/2 as potential prognostic markers in bladder cancer. *Br. J. Cancer* **2015**, *113*, 282–289. [CrossRef]

46. Masuda, T.A.; Inoue, H.; Nishida, K.; Sonoda, H.; Yoshikawa, Y.; Kakeji, Y.; Utsunomiya, T.; Mori, M. Cyclin-dependent kinase 1 gene expression is associated with poor prognosis in gastric carcinoma. *Clin. Cancer Res.* **2003**, *9*, 5693–5698. [PubMed]

47. Kitajima, S.; Kudo, Y.; Ogawa, I.; Bashir, T.; Kitagawa, M.; Miyauchi, M.; Pagano, M.; Takata, T. Role of Cks1 overexpression in oral squamous cell carcinomas: Cooperation with Skp2 in promoting p27 degradation. *Am. J. Pathol.* **2004**, *165*, 2147–2155. [CrossRef] [PubMed]

48. Shapira, M.; Ben-Izhak, O.; Bishara, B.; Futerman, B.; Minkov, I.; Krausz, M.M.; Pagano, M.; Hershko, D.D. Alterations in the expression of the cell cycle regulatory protein cyclin kinase subunit 1 in colorectal carcinoma. *Cancer* **2004**, *100*, 1615–1621. [CrossRef] [PubMed]

49. Zhang, Y.; Chen, Y.; You, F.; Li, W.; Lang, Z.; Zou, Z. Prognostic and clinicopathological significance of Cks1 in cancer: Evidence from a meta-analysis. *J. Cell Physiol.* **2019**, *234*, 13423–13430. [CrossRef]

50. Shapira, M.; Ben-Izhak, O.; Linn, S.; Futerman, B.; Minkov, I.; Hershko, D.D. The prognostic impact of the ubiquitin ligase subunits Skp2 and Cks1 in colorectal carcinoma. *Cancer* **2005**, *103*, 1336–1346. [CrossRef]

51. Slotky, M.; Shapira, M.; Ben-Izhak, O.; Linn, S.; Futerman, B.; Tsalic, M.; Hershko, D.D. The expression of the ubiquitin ligase subunit Cks1 in human breast cancer. *Breast Cancer Res.* **2005**, *7*, R737–R744. [CrossRef] [PubMed]

52. Xu, L.; Fan, S.; Zhao, J.; Zhou, P.; Chu, S.; Luo, J.; Wen, Q.; Chen, L.; Wen, S.; Wang, L.; et al. Increased expression of Cks1 protein is associated with lymph node metastasis and poor prognosis in nasopharyngeal carcinoma. *Diagn. Pathol.* **2017**, *12*, 2. [CrossRef] [PubMed]

53. Biodiscovery LLC. *Nexus Copy Number Version 7.5 User Manual*; Biodiscovery LLC: Ann Arbor, MI, USA, 2014.

54. Scott, A.T.; Weitz, M.; Breheny, P.J.; Ear, P.H.; Darbro, B.; Brown, B.J.; Braun, T.A.; Li, G.; Umesalma, S.; Kaemmer, C.A.; et al. Gene Expression Signatures Identify Novel Therapeutics for Metastatic Pancreatic Neuroendocrine Tumors. *Clin. Cancer Res.* **2020**, *26*, 2011–2021. [CrossRef]

55. Lai, Y.P.; Wang, L.B.; Wang, W.A.; Lai, L.C.; Tsai, M.H.; Lu, T.P.; Chuang, E.Y. iGC-an integrated analysis package of gene expression and copy number alteration. *BMC Bioinform.* **2017**, *18*, 35. [CrossRef] [PubMed]